Thermochemical Properties of the Ammonia−Water Ionized Dimer Probed by Ion−Molecule Reactions

Safwat Abdel Azeim and Guillaume van der Rest*

Laboratoire des Mécanismes Réactionnels, CNRS UMR 7651, Ecole Polytechnique, 91128 Palaiseau Cedex, France

Received: October 7, 2004; In Final Form: December 21, 2004

The thermochemical properties of some small clusters such as the $(H_2O)_2^{\bullet+}$ dimer have already been investigated by both experimental and theoretical methods. The recent method to selectively prepare the ammonia−water ionized dimer $[NH_3, H_2O]^{\bullet+}$ (and not its proton transfer isomer $[NH_4^+, OH^\bullet]$) allowed us to study its chemical reactivity. This study focuses on the charge and proton transfer pathways: Ion−molecule reactions in the cell of an FT-ICR mass spectrometer were carried out with a range of organic compounds. Examination of the reactivity of the $[NH_3, H_2O]^{\bullet+}$ ionized dimer versus ionization energy and proton affinity of the neutral reagents shows a threshold in the reactivity in both instances. This leads to a bracketing of thermochemical properties related to the dimer. From these experiments and in agreement with ab initio calculations, the adiabatic recombination energy of the $[NH_3, H_2O]^{\bullet+}$ dimer was evaluated at -9.38 ± 0.04 eV. The proton affinity bracketing required the reevaluation of two reference gas-phase basicity values. The results, in good agreement with the calculation, lead to an evaluation of the proton affinity of the $[NH_2^\bullet, H_2O]$ dimer at 204.4 $\pm$ 0.9 kcal mol^{-1}. These two experimental values are respectively related to the ionization energy of $NH_3^{\bullet+}$ and to the proton affinity of $NH_2^\bullet$ by the difference in single water molecule solvation energies of ionized ammonia, of neutral ammonia, and of the $NH_2^\bullet$ radical.

Introduction

A couple of years ago, our group devised a method to produce and isolate the ionized ammonia−water mixed dimer in the cell of a Fourier transform ion cyclotron resonance (FT-ICR) mass spectrometer,[1] by using the reaction of ionized formamide or ionized hydroxyaminocarbene with water (eqs 1 and 2). Although the properties of isolated neutral ammonia−water dimer have been investigated spectroscopically in matrixes[2,3] and in molecular beams[4−6] and well-characterized by theoretical calculations,[7,8] those of the ionized dimer had only been predicted by means of theoretical calculations.[9,10] These latter results, refined by higher-level calculations,[1] showed that two stable structures can exist for the $[NH_3, H_2O]^{\bullet+}$ dimer (Chart 1): **1a**, the most stable, corresponds to a hydrogen-bonded structure in which both the charge and the radical are located on the NH_3 moiety; **1b**, 4.8 kcal mol^{-1} less stable than **1a**, corresponds to a proton transfer structure $[NH_4^+, OH^\bullet]$. Collision-induced dissociation experiments showed that the ions produced by reactions 1 and 2 are of structure **1a**.[1]

$$HCONH_2^{\bullet+} + H_2O \rightarrow [NH_3, H_2O]^{\bullet+} + CO \qquad (1)$$

$$HOCNH_2^{\bullet+} + H_2O \rightarrow [NH_3, H_2O]^{\bullet+} + CO \qquad (2)$$

A related ionized dimer, the ionized water homodimer, has been extensively studied in the past years, because it is easy to produce either by photoionization of water dimers in a supersonic jet[11,12] or by consecutive exchange of xenon atoms by water molecules in the ionized xenon dimer.[13,14] The latter method led to a comprehensive study of the gas-phase reactivity of the ionized water dimer.[14] The recombination energy (RE) of the ionized water dimer was bracketed on the basis of the charge transfer reactions (or absence of these reactions) with a set of reference molecules. The lack of similar experimental data for the $[NH_3, H_2O]^{\bullet+}$ dimer was a motivation for the current work, which will make use of a similar methodology to determine two thermochemical properties related to this dimer: the adiabatic recombination energy of the ionized $[NH_3, H_2O]^{\bullet+}$ dimer (which is the opposite of the adiabatic ionization energy of the $[NH_3, H_2O]$ dimer) and the proton affinity of the $[NH_2^\bullet, H_2O]$ solvated radical.

CHART 1

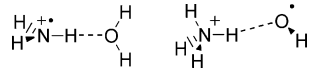

1a **1b**

Another motivation for this work is that the $[NH_3, H_2O]^{\bullet+}$ dimer can be considered as a prototype of hydrogen-bridged radical cations. These odd-electron complexes, built of two moieties, one an even-electron species, the other one an odd-electron species, linked by a proton, present a very diverse reactivity. A first set of reactions arises from the proton-bound structure of these dimers. A quite obvious reactivity for these dimeric species is the occurrence of ligand exchange with various neutral molecules. The exchanged moiety can be either the even-electron species or the radical species, depending on the relative proton affinities of the moieties. For instance, the major reaction of the ionized enol−water dimer (formed itself by the reaction of the enol radical cation with *tert*-butyl alcohol) is the exchange of the water molecule by *tert*-butyl alcohol (eq 3).[15] A further reaction of the ionized enol−*tert*-butyl alcohol dimer is the exchange of the $CH_2CHO^\bullet$ radical leading to the formation of a protonated *tert*-butyl alcohol dimer (eq 4). A second reactivity typical of proton-bound cations, which has been abundantly studied, is a catalyzed isomerization occurring within the complex: one moiety can help in the transport of a

* gvdr@dcmr.polytechnique.fr.

10.1021/jp045425c CCC: $30.25
Published on Web 02/23/2005

proton leading to an isomerization within the complex. Catalyzed isomerizations are also observed within hydrogen-bridged radical cations.[16−20] A typical reaction is the isomerization of ionized methanol into its more stable α-distonic isomer catalyzed by water, which proceeds through two intermediate hydrogen-bridged radical cations[16,21,22] (eq 5).

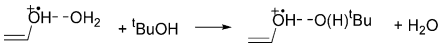

(3)

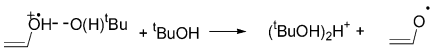

(4)

$$CH_3OH^{\bullet+} + H_2O \rightarrow [CH_3OH^{\bullet+}\cdots OH_2] \rightarrow [^{\bullet}CH_2OH_2^{+}\cdots OH_2] \rightarrow {}^{\bullet}CH_2OH_2^{+} + H_2O \quad (5)$$

On the other hand, the radical cation nature of the complex can be evidenced by the appearance of three-electron/two-center ($3e^-/2c$) bonds or by charge transfer reactions. For instance, in the reaction of ionized acetaldehyde with methanol, the 1,3-H-transport isomerization is made possible by the initial formation of a $3e^-/2c$ bond which lies only slightly higher in energy than the proton-bound structure.[23] Other radical-type reactions such as H$^{\bullet}$-atom transfer are also possible. For instance, such a radical shift is involved in the second step of the reaction leading to the overall isomerization of the acetamide radical cation catalyzed by benzonitrile[24] (eq 6). Finally, the radical cations moiety can retain its intrinsic reactivity. This is the case for the water-solvated distonic ion $^{\bullet}CH_2CH_2O(H)CH_3^{+}$ which reacts by I$^{\bullet}$ abstraction with allyl iodide,[25] a reaction typical of its radical site (eq 7). It is also the case for the water-solvated enol ion, which undergoes a cycloaddition−cycloreversion reaction with isobutene[15,25] (eq 8).

$$C_6H_4{}^{\bullet}CN\cdots H^{+}-O{=}C(NH_2)CD_3 \rightarrow C_6H_4DCN\cdots HOC(NH_2){=}CD_2^{\bullet+} \quad (6)$$

$$[^{\bullet}CH_2CH_2O(H)CH_3^{+}, H_2O] + CH_2CHCH_2I \rightarrow [ICH_2CH_2O(H)CH_3^{+}, H_2O] + CH_2CHCH_2^{\bullet} \quad (7)$$

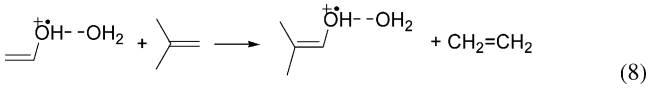

(8)

The investigations underway on the reactivity of the $[NH_3, H_2O]^{\bullet+}$ dimer led to the grouping of its reactions into five classes which follow the above scheme: the first two are typical of the proton-bound structure of the dimer, whereas the last three rely on the radical-cation nature of the dimer.

(1) Ligand Exchange Reactions (LS). The $[NH_3, H_2O]^{\bullet+}$ dimer reacts with various neutral molecules by simple ligand exchange.[1] This can be the only reaction product, such as in the reaction with carbon disulfide (eq 9). In the case of alkenes, the ligand switch can be followed by a collapse to a covalent bond, leading to the formation of a *β*-distonic ion (eq 10). The formation of such distonic ions is exothermic, and it is the major pathway for most alkene-containing molecules.

$$[NH_3, H_2O]^{\bullet+} + CS_2 \rightarrow [NH_3, CS_2]^{\bullet+} + H_2O \quad (9)$$

$$[NH_3, H_2O]^{\bullet+} + CH_2{=}CH_2 \rightarrow {}^{+}H_3N{-}CH_2CH_2^{\bullet} + H_2O \quad (10)$$

(2) Proton Transfer Reactions (PT). When the proton affinity of the reactant neutral is sufficiently high, it can abstract a proton from the dimer through an intermediate three-body complex (eq 11). This pathway is discussed in the present article: The reaction of the $[NH_3, H_2O]^{\bullet+}$ dimer with a range of reference neutral bases is used to bracket the proton affinity of the $[NH_2^{\bullet}, H_2O]$ solvated radical.

$$[NH_3, H_2O]^{\bullet+} + B \rightarrow [NH_3, H_2O, B]^{\bullet+} \rightarrow BH^{+} + [NH_2^{\bullet}, H_2O] \text{ or } BH^{+} + NH_2^{\bullet} + H_2O \quad (11)$$

(3) Charge Transfer Reactions (CT). These reactions are similar to the proton transfer reactions except for an electron transfer to a radical cation: They occur when the $[NH_3, H_2O]^{\bullet+}$ dimer reacts with an electron donor species of sufficiently low ionization energy (eq 12). This reaction is the other reaction pathway discussed in the present article. In a manner similar to the determination of the proton affinity of the $[NH_2^{\bullet}, H_2O]$ solvated radical, the reactions of the $[NH_3, H_2O]^{\bullet+}$ dimer with a range of neutral molecules of known ionization energies is used to bracket the adiabatic ionization energy of the $[NH_3, H_2O]$ neutral dimer.

$$[NH_3, H_2O]^{\bullet+} + N \rightarrow [NH_3, H_2O, N]^{\bullet+} \rightarrow N^{\bullet+} + [NH_3, H_2O] \text{ or } N^{\bullet+} + NH_3 + H_2O \quad (12)$$

(4) Hydrogen Abstraction Reactions (HA). This reaction is also related to the odd-electron properties of the dimer. An example of such reactions is the exothermic reactions with long-chain aldehydes, a minor pathway of which leads to the appearance of $[NH_4, H_2O]^{+}$ and NH_4^{+} cations (eq 13).[26]

$$[NH_3, H_2O]^{\bullet+} + CH_3(CH_2)_2CHO \rightarrow [NH_4, H_2O]^{+} + CH_3(CH_2)_2CO^{\bullet} \rightarrow NH_4^{+} + H_2O + CH_3(CH_2)_2CO^{\bullet} \quad (13)$$

(5) Ammonia-Solvated Fragmentation-Type Reactions (FR). In a number of instances, a product possessing the structure of an ammonia-solvated fragment of the reagent molecule was observed. Different pathways could be involved in this class of reactions, which have not yet been investigated fully, except for the case of the reactions of long-chain ketones and aldehydes. In this latter case, the major and often only reaction product is a McLafferty rearrangement product solvated by an ammonia molecule (eq 14).[26]

$$[NH_3, H_2O]^{\bullet+} + CH_3(CH_2)_2CHO \rightarrow [NH_3, CH_2{=}CHOH]^{\bullet+} + CH_2CH_2 + H_2O \quad (14)$$

In the present work, the aim was to use ion−molecule reactions to determine two thermochemical values related to the dimer. Therefore, the focus has been put on pathways (2) and (3). To obtain these thermochemical values, it has been proven necessary to investigate the ion−molecule reactions of the dimer with a range of neutral molecules, for which the different pathways are in competition. For this reason, a number of other reaction products have been observed and are mentioned in the experimental results, but a full discussion of these results is out of the scope of this article.

Experimental and Computational Procedures

Ion−Molecule Reactions. The bimolecular reactions of ions were examined in a Bruker CMS-47X FT-ICR mass spectrom-

eter[27] equipped with an external ion source[28] and an infinity cell.[29] The reagents were all commercially available and used without further purification. Liquid reagents introduced through the leak valve assembly were thoroughly degassed through several freeze−pump−thaw cycles. In a typical experiment, oxamide is introduced in the direct insertion probe of the external source of the mass spectrometer. The ionization of oxamide leads, among other ions, to the formation of the $H_2NCOH^{\bullet+}$ *m/z* 45 ionized carbene ion.[30]

A difficulty in the protocol used for these experiments is that the $[NH_3, H_2O]^{\bullet+}$ dimer is prepared in the cell of the FT-ICR mass spectrometer by an ion−molecule reaction with water. Three different protocols were set up to perform the ion−molecule reactions, depending on the neutral of interest and on the types of results that are being looked for:

(i) Static Pressures of Water and Argon; Pulsed Introduction of the Neutral of Interest. This is the same experimental procedure as detailed in ref 1. Water and argon are introduced through leak valves. The pressure is set at 4×10^{-8} mbar for water. Argon, used as a bath gas to thermally cool the initially translationally excited ions, was added up to a total pressure of 2×10^{-7} mbar. The $H_2NCOH^{\bullet+}$ *m/z* 45 is selectively isolated by the use of on-resonance radio frequency (rf) ejection of all unwanted ions. The ammonia−water ionized dimer is produced by an ion−molecule reaction of $H_2NCOH^{\bullet+}$ with water taking place for 5 s. After this delay, the $[NH_3, H_2O]^{\bullet+}$ *m/z* 35 product ion is selected by an rf ejection of the $H_2NCOH^{\bullet+}$ *m/z* 45 ion. The reagent gas is then introduced by means of a solenoid pulsed valve. The peak pulse pressure is usually around a few 10^{-6} mbar, and the pulses can be repeated up to five times, separated by 0.5 s. This procedure led to qualitative results on the ion−molecule reactions of the ammonia−water dimer, but it presents some shortcomings: There is only a crude control on the pressure of the introduced gas, and it is not possible to perform time-dependent experiments.

(ii) Static Pressures of Water and of the Neutral of Interest. This procedure leads to kinetic measurements for the ion−molecule reactions of the ammonia−water dimer. Water and the neutral of interest are introduced through leak valves: the pressures are set at $(1-3) \times 10^{-8}$ mbar for the neutral of interest, and water is added up to a total pressure of 4×10^{-7} mbar. With such a high pressure of water, conversion of the externally produced $H_2NCOH^{\bullet+}$ is achieved after a 1.5-s delay, and there is no need to add argon as a thermalization gas bath. (It was shown that the ammonia−water ionized dimer does not react further with water; therefore, water does not interfere with the primary reactions of the dimer. Water should nevertheless be considered a possible reactant when secondary products are formed.) After this delay, the dimer is selectively isolated by rf ejection of all unwanted ions. It should be pointed out that reactions with the other neutral gas can occur during this first reaction step: either the initial carbene ion can react with the neutral gas or the dimer can itself react with the neutral gas. Both of these reactions result in a decrease in the yield of rf-isolated dimer; therefore, experimental conditions were optimized to a high ratio between the pressure of the water vapor and that of the reagent of interest.

By varying the delay between the selection of the ionized dimer and the excitation-detection step, one can plot the intensities of the parent ion and of the reaction product relative to the total ion intensity as a function of time. From these plots, experimental rate constants and branching ratios between competing reaction pathways are determined. The experimental rate constants are indicated after correction of the read pressure by the gauge sensitivity for the neutral under consideration. For most neutrals for which the sensitivity is not known, the empirical relationship between gauge sensitivity and polarizability established by Bartmess[31] was used. In the absence of experimental data, the polarizability was computed following the method by Miller.[32] The efficiencies of the reactions are reported as the ratio of the experimental rate constant to the calculated collision rate constant, following the method of Su and Chesnavich.[33]

(iii) Static Pressures of Water and of the Neutral of Interest with Continuous Ejection of $H_2O^{\bullet+}$ or H_3O^+. In the cases where the reaction rates are very slow (half-reaction on the order of 5 s), an experimental artifact appeared in the spectra due to the high pressure of water in the instrument. The high-voltage ion transfer system of the apparatus leads to some ionization of the water-bath gas, which results in a slow bleeding of $H_2O^{\bullet+}$ into the cell of the mass spectrometer. These ions can undergo an $H^{\bullet}$-atom transfer with neutral water leading to the formation of H_3O^+. These two ions are respectively very efficient electron acceptors ($IE(H_2O) = 12.62$ eV[34]) and proton donors ($PA(H_2O) = 165.0$ kcal mol^{-1} [35]), and thus, they interfere in the measurement of charge transfer and proton transfer reactions, because they can also react with the gas of interest. To circumvent this problem, most reactions were repeated three times: in a first experiment, the procedure described above is followed; in a second experiment, the reaction delay was replaced by a continuous rf ejection at the mass of $H_2O^{\bullet+}$ (*m/z* 18.010) of the same duration; and in a third experiment, the continuous ejection was done at the mass of H_3O^+ (*m/z* 19.018). Comparison of the three results allowed us to ascertain that slowly occurring charge transfer or proton transfer originated from a reaction of the $[NH_3, H_2O]^{\bullet+}$ and not from this artifact.

Calculations. The *Gaussian 98*[36] program package was used for calculations to determine the theoretical values for the thermochemical values determined in this article. In a first step, the G3(MP2)[37] method was used: following an MP2/6-31G** optimization, two single-point calculations, one with a large basis set, and the other with QCISD(T) electron correlation, were conducted to obtain the energies. The frequencies, used for thermochemical corrections at 298 K, were evaluated at the MP2/6-31G** level of the theory and scaled by a factor of 0.93. To check the accuracy of the energy obtained by the G3 composite method on these small open-shell systems, a CCSD(T)/aug-cc-pVTZ single-point calculation was run on both the MP2/6-31G** and B3LYP/6-31G** optimized geometries.

Results

As described in the Introduction, the ammonia−water ionized dimer reacts with neutral molecules through a number of different and often competitive reaction pathways. A typical example is the reaction with 2-hexanone for which three reaction pathways are observed. At 5-s reaction time, which is about half-reaction time (Figure 1), five different products can be identified: $[CH_2{=}C(CH_3)O^{\bullet}, NH_4^+]$, [2-hexanone, NH_4^+], 2-hexanone$^{\bullet+}$, NH_4^+, and $(2\text{-hexanone})_2H^+$. From the semilogarithmic kinetic plot (Figure 2), it is apparent that $[CH_2{=}C(CH_3)O^{\bullet}, NH_4^+]$ (pathway FR), 2-hexanone$^{\bullet+}$ (pathway CT), and NH_4^+ (pathway HA) follow parallel evolutions at early reaction delays, indicating that these are primary reaction products, whereas [2-hexanone, NH_4^+] and $(2\text{-hexanone})_2H^+$ appear at later delays, showing that these are secondary products. The decay of $[CH_2{=}C(CH_3)O^{\bullet}, NH_4^+]$ after 5 s suggests that

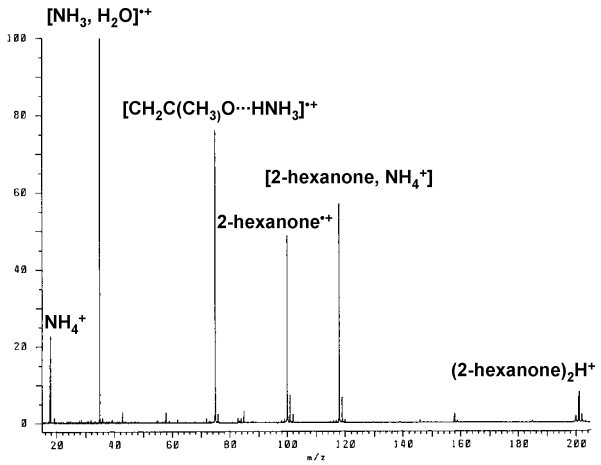

Figure 1. Mass spectrum of the products of the reaction between $[NH_3, H_2O]^{\bullet+}$ and 2-hexanone ($P = 2 \times 10^{-8}$ mbar), after 5 s, with continuous ejection of m/z 19.

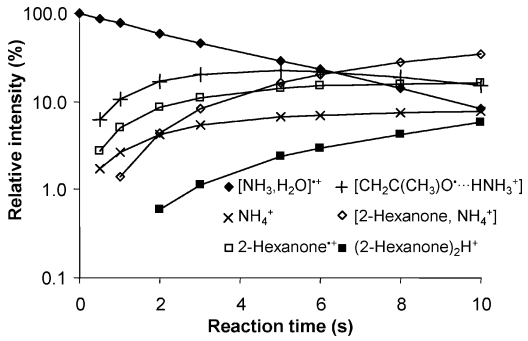

Figure 2. Normalized relative intensities (semilog plot) of the ions observed for the reaction of $[NH_3, H_2O]^{\bullet+}$ with 2-hexanone ($P = 2 \times 10^{-8}$ mbar), with continuous ejection of H_3O^+, as a function of time.

two successive ligand-switching reactions occur:

$$[CH_2{=}C(CH_3)O^{\bullet}, NH_4^+] + \text{2-hexanone} \rightarrow [\text{2-hexanone}, NH_4^+] \quad (15)$$

$$[\text{2-hexanone}, NH_4^+] + \text{2-hexanone} \rightarrow (\text{2-hexanone})_2H^+ \quad (16)$$

Charge Transfer Reactions. To probe the CT channel, reactions of $[NH_3, H_2O]^{\bullet+}$ with a number of reference compounds of known ionization energies were conducted. The aim was to undertake an ionization energy bracketing experiment, similar to the standard bracketing experiments used for the measurement of proton affinities. Only reagents with no alkene bond were chosen: early work[1] and currently unpublished work showed that alkene compounds react almost exclusively by ligand-switching reactions even when other pathways could exist. It was therefore of little interest to study the charge transfer mechanism on these compounds. In a first step, qualitative results were obtained by the use of pulsed gas introduction following the first protocol described above (Table 1). An interesting reaction that is worth notice for this series of reactants is that of some halobenzenes and of bromoethylene: a channel is open that leads to a substitution of one halogen atom by $NH_3^{\bullet+}$. Such reactions have been described both in the photoionization[38−40] and in the ion−molecule reactions[41,42] of halobenzene−ammonia clusters.

Because as expected, the ionization energy (IE) of the reagents is a major criterion for the charge transfer mechanism, this study focused on compounds within a narrow ionization energy range (9.2−9.5 eV). In this range, the results with the pulsed-valve method were often hard to interpret and ambiguous, mostly because without a kinetic plot, it is hard to discriminate between primary and secondary reaction products. To improve the quality of the results, a new protocol, using static pressures of the reactant gas was developed (see Methods section). Unfortunately, volatile and commercially available neutral compounds in this ionization energy range are scarce, and for most of these, the ionization energy is not known with good precision. It was nevertheless possible to cover this energy range with sufficient accuracy, using the static pressure protocols. The results are summarized in Table 2.

Proton Transfer Reactions. Following the same methodology as the one used for charge transfer reactions, the proton transfer channel (PT) was probed by reaction with a series of compounds of varying proton affinities. For these experiments, it was necessary to use compounds with a sufficient proton affinity, but with sufficiently high ionization energy so that the charge transfer channel would not interfere with the proton transfer channel. As for the previous series of experiments, alkene compounds could not be used. These two criteria restricted the choice of neutral reagents available in this proton affinity range to a short list. The results are presented in Table 3.

One striking feature of this results table is the appearance, even for bases with a PA lower than the threshold for proton transfer, of a minor channel corresponding to the loss of $NH_2^{\bullet}$.

Discussion

Charge Transfer Reactions. The results, presented in Tables 1 and 2, clearly indicate a threshold in the IE of the neutral for the charge transfer to take place: charge transfer occurs for 2-pentanone (IE 9.38 eV) but not for benzenacetonitrile (IE 9.39 eV). This could be interpreted in terms of a bracketing experiment: the charge transfer is observed when the overall reaction is exothermic, and provided that no significant energy barrier exists, the nonoccurrence of charge transfer indicates an endothermic reaction. But in order to validate this interpretation, one needs at first to answer three questions: what type of charge transfer mechanism occurs, which are the species involved in this bracketing, and finally, could there be a significant energy barrier?

The charge transfer reaction rates, on the order of 6×10^{-10} $cm^3\ s^{-1}$ $molecule^{-1}$ are much lower than the collision rate constant (3.2×10^{-9} $cm^3\ s^{-1}$ $molecule^{-1}$ for cyclobutanone). For a vertical charge transfer to occur, the neutral and the ionized species are not required to interact through an intermediate interacting complex, because long-range transfers would be possible. In those conditions, the rate constant could be higher than the collision rate. Thus, a reaction rate constant lower than the collision rate constant is an indication that the charge transfer takes place during the lifetime of an intermediate ion−molecule complex. By definition, an adiabatic charge transfer takes place between the lowest vibrational and rotational state of the neutral molecule and the lowest vibrational and rotational state of the ionized molecule, thus at a 0 K temperature. In the instrument used for this work, the reactions take place at 298 K; thus, both the neutral and ionized molecules are thermally excited. Lias and Ausloos showed,[43] by taking into account the various heat capacities, that as long as differences are considered, the enthalpy difference at a finite temperature for a charge transfer reaction is approximately equal to the difference between the adiabatic ionization energies. Therefore, as long as the bracket-

TABLE 1: Occurrence (+) and Nonoccurrence (−) of Different Pathways for the Reaction of $[NH_3, H_2O]^{\bullet+}$ with a Series of Compounds Pulsed into the Cell of an FT-ICR Mass Spectrometer

compound	IE (eV)[a]	CT[b]	PT[b]	LS[b]	HA[b]	other fragmentations[c]
bromobenzene	9.00 ± 0.03	+	−	−	−	
1,2-dichlorobenzene	9.06 ± 0.02	+	−	−	−	*m/z* 128 (+ $NH_3^{\bullet+}$, −Cl$^\bullet$, −H_2O)
chlorobenzene	9.07 ± 0.02	+	−	−	−	*m/z* 93 (+$NH_3^{\bullet+}$, −Cl$^\bullet$, −H_2O)
3,3-dimethyl-2-butanone	9.14 ± 0.03	+	−	−	−	
fluorobenzene	9.20 ± 0.01	+	−	+	−	
3-methyl-2-pentanone	9.21 ± 0.01	+	−	+	−	
benzene	9.243780 ± 0.00007	+	−	+	−	
1,3,5-trifluorobenzene	9.6 ± 0.1	−	−	+	−	
bromoethylene	9.82 ± 0.03	−	−	+	+[d]	*m/z* 44 (+$NH_3^{\bullet+}$, −Br$^\bullet$, −H_2O)

[a] Ionization energies from ref 34. [b] Reaction channels described in the text: CT (charge transfer), PT (proton transfer), LS (ligand switching), HA (hydrogen abstraction). [c] For the other major reaction products observed: measured mass (assumed neutral losses from the [M, NH_3, H_2O]$^{\bullet+}$ complex leading to the fragmentation). [d] Formation of NH_4^+.

TABLE 2: Rate Constants and Branching Ratios of the Different Pathways Observed for the Reaction of $[NH_3, H_2O]^{\bullet+}$ with a Series of Compounds of Ionization Energy in the 9.2−9.5-eV Range, Introduced at a Static Pressure into the Cell of an FT-ICR Mass Spectrometer

compound	IE (eV)[a]	exptl rate constant (cm^3 s^{-1} $molecule^{-1}$)	branching ratios CT[b]	PT[b]	LS[b]	HA[b]	other fragmentations[c]
cyclopentanone	9.26 ± 0.01	7.2×10^{-10}	75				*m/z* 72 (−$C_2H_5^\bullet$, −H_2O) 25
5-methyl-2-hexanone	9.284 ± 0.005	7.6×10^{-10}	35			10	*m/z* 75 (−C_4H_8, −H_2O) 55
1,2-dimethoxyethane	9.3 ± 0.1	3.2×10^{-10}	<5	25			*m/z* 58 (−CH_3OH, −NH_3, −H_2O) 40; *m/z* 75 (−CH_3OH, −H_2O) 30
3-pentanone	9.31 ± 0.02	1.1×10^{-9}	100				
1,3-difluorobenzene	9.33 ± 0.02	1.1×10^{-9}	73		27		
iodoethane	9.349 ± 0.001	9.8×10^{-10}	60		7	33	
cyclobutanone	9.35 ± 0.01	6.3×10^{-10}	51			21	*m/z* 59 (−C_2H_4) 22
2-hexanone	9.35 ± 0.06	1.3×10^{-9}	26			16	*m/z* 75 (−C_3H_6, −H_2O) 58
2-pentanone	9.38 ± 0.06	5.7×10^{-10}	43			41	*m/z* 75 (−C_2H_4, −H_2O) 16
phenylacetonitrile	9.39 ± 0.07	1.1×10^{-10}				100	
tetrahydrofuran	9.40 ± 0.02	6.1×10^{-10}				34	*m/z* 91 (−$NH_2^\bullet$) 40; *m/z* 61 (−C_2H_4, −H_2O) 14; *m/z* 42 12
2-fluoropyridine	9.4 ± 0.1	1.5×10^{-9}		100			
3-nitrotoluene	9.5 ± 0.1	no reaction					
benzaldehyde	9.50 ± 0.08	6.7×10^{-10}			60		*m/z* 125 (−$NH_2^\bullet$) 40
diethyl ether	9.51 ± 0.03	5.6×10^{-10}				39	*m/z* 93 (−$NH_2^\bullet$) 39; *m/z* 62 (−$C_2H_5^\bullet$, −H_2O) 22

[a] Ionization energies from ref 34. [b] Reaction channels described in the text: charge transfer (CT), proton transfer (PT), ligand switching (LS), hydrogen abstraction (HA). [c] For the other major reaction products observed: measured mass (assumed neutral losses from the [M, NH_3, H_2O]$^{\bullet+}$ complex leading to the fragmentation), branching ratio.

TABLE 3: Rate Constants and Branching Ratios of the Different Pathways Observed for the Reaction of $[NH_3, H_2O]^{\bullet+}$ with a Series of Compounds of Proton Affinities in the 198−215 kcal mol^{-1} Range, Introduced at a Static Pressure into the Cell of an FT-ICR Mass Spectrometer

compound	PA (kcal mol^{-1})	exptl rate constant (cm^3 s^{-1} $molecule^{-1}$)	branching ratios CT[a]	PT[a]	LS[a]	HA[a]	other fragmentations[b]
methyl propanoate	198.4[c]	1.2×10^{-9}				75	*m/z* 107 (−$NH_2^\bullet$) 25
methyl butanoate	199.9[c]	2.4×10^{-10}				75	*m/z* 121 (−$NH_2^\bullet$) 25
4-fluoroacetophenone	203.8[d] (205.2[c])	no reaction					
1,2-dimethoxyethane	205.1[c]	3.2×10^{-10}	<5	25			*m/z* 58 (−CH_3OH, −NH_3, −H_2O) 40; *m/z* 75 (−CH_3OH, −H_2O) 30
N-methyl formamide	205.9[d] (203.5[c])	7.1×10^{-10}		69		12	*m/z* 78 (−$NH_2^\bullet$) 19
tert-butyl isocyanide	208.1[c]			100			
2-fluoropyridine	211.0[c]	1.5×10^{-9}		100			

[a] Reaction channels described in the text: charge transfer (CT), proton transfer (PT), ligand switching (LS), hydrogen abstraction (HA). [b] For the other major reaction products observed: measured mass (assumed neutral losses from the [M, NH_3, H_2O]$^{\bullet+}$ complex leading to the fragmentation), branching ratio. [c] Proton affinities from ref 35. [d] Remeasured proton affinities (this work, see discussion).

ing probes the lowest-energy channel for the charge transfer pathway, the measurement of an exothermicity threshold for the charge transfer is approximately equivalent to the measurement of an adiabatic ionization energy threshold.

As indicated in eq 11, the CT reaction channel can lead to two different reaction products: formation of an [NH_3, H_2O] neutral dimer or of two independent neutral molecules NH_3 + H_2O. As described in the thermodynamic cycle for this system (Scheme 1), the first pathway is slightly more exothermic than the second one by $\Delta H_{solv}(NH_3)$ which has been evaluated by high-level ab initio calculations[7] at about −4.1 kcal mol^{-1} (0.18 eV). As the neutral molecules cannot be observed in the FT-ICR mass spectrometer, there is no direct experimental proof that the threshold observed is that for the formation of the [NH_3, H_2O] neutral dimer. To answer this question, for which more experimental evidence will be developed later, ab initio calcula-

SCHEME 1

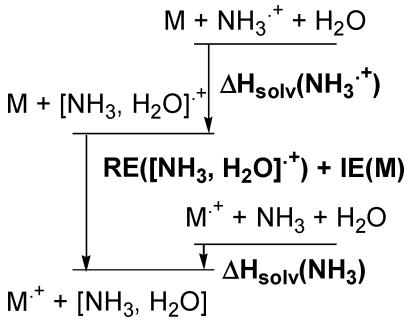

tions of the various charge transfer exit points were performed (Table 4 and Figure 3), considering only the structures that were found as the most stable ones in refs 1, 7, and 9. The various levels of calculation that have been used (G3(MP2), CCSD(T)/aug-cc-pVTZ//MP2/6-31G**, and CCSD(T)/aug-cc-pVTZ//B3LYP/6-31G**) lead to consistent results for the various structures, except for the vertical transition energies. The observed experimental threshold (9.38 eV) is in much better agreement with the formation of the [NH_3, H_2O] neutral dimer (9.34−9.41 eV depending on the method) than with the formation of dissociated NH_3 and H_2O (computed at 9.07−9.13 eV). These remarks hold true within a system that does not interact with its surroundings, which is a good approximation for a short-lived intermediate complex in the low-pressure conditions of an FT-ICR cell, where collisional relaxation of the intermediate complex is limited. After dissociation of the intermediate complex, the neutral [NH_3, H_2O] dimer will eventually itself dissociate, because the low binding energy of this complex cannot compensate for the entropy gain.

The last point goes to the basis of bracketing experiments used for the measurement of thermochemical data: the bracketing is significant only if there is no energy barrier associated to the measured transfer, because the only observed parameter is the occurrence or nonoccurrence of the reaction. The occurrence of a reaction indicates an exothermic reaction, but the nonoccurrence can indicate either an endothermic reaction or an energy barrier higher than the entry point on the way to the reaction products. For proton transfer reactions, it is generally assumed that the proton transfer barriers are small and well below the interaction energy of the intermediate complex. Bracketing methods are standard methods for the measurement of proton affinities in the gas phase when one of the neutrals is not readily available in the gas phase[44] and the results agree well with those from other methods. The literature is much less abundant for the measurement of ionization energies by bracketing experiments.[45−47] A generally accepted requirement for these measurements is that there is no significant barrier as long as the charge transfer does not induce a major reorganization of the geometry of the molecules. Unfortunately, this is not the case for the ammonia−water dimer where the water and ammonia molecules rotate between the neutral and ionized structures (Figure 3a,b). An indication for the presence of a barrier for charge transfer could be observed by varying the natures of the species between which the charge transfer takes place: if a barrier was present, its level would depend on the chemical nature of the compounds involved in the charge transfer, possibly leading to a discrepancy in the bracketing measurement. The different chemical functions used for this bracketing experiment (ketones, ethers, nitriles) indicate a similar value for the bracketing of the recombination energy, but because there are only a few reference bases with similar chemical functions close to the threshold, it is not possible on the basis of the experiments alone to conclude the nonexistence of a significant barrier on the charge transfer pathway. Once again, only the agreement between the calculations and the experimental results support the hypothesis that there is no barrier higher than the entry point on the charge transfer channel for this system, although there is a considerable rearrangement. This can be rationalized if one considers that, even if there is a complete geometry change, these modifications only involve two species linked by hydrogen bonds and not covalent bonds. Therefore, the net effect on the system energetics is rather limited.

A last issue is the presence of competing reaction channels. These channels put an experimental limitation on the detection of the nonoccurrence of a charge transfer reaction. If there were no competing reactions, a criterion for the nonoccurrence of a reaction would be defined as the absence of any reaction product after a given time with a given reactant pressure. In the presence of competing reactions, it is not always possible to reach these conditions, because a reaction occurring much more rapidly than the charge transfer puts a limit on the time frame and pressure range for which the observation is feasible. This problem was circumvented through the use of reagents for which no major competing reaction channels were expected, thus removing from the list of reagents the alkenes for which the ligand-switching channel is known to be predominant. But removing all reagents for which no other competing reaction was observed would be too restrictive: in the case of the current work, only 3-nitrotoluene could be considered a valid reagent.

Within the limits pointed out in the three previous points, it can be concluded that these experiments lead to a measurement of the adiabatic recombination energy of the ammonia−water ionized dimer. A last point to consider is that the IEs of reference neutral compounds are known with very differing accuracies. If one looks at the reference compounds for which the IE is known with accurate precision and that closely bracket the RE of [NH_3, H_2O]$^{\bullet+}$, it is can be seen that the IE of iodoethane (9.349 ± 0.001 eV) is a lower limit for the RE of [NH_3, H_2O]$^{\bullet+}$. On the upper side, the IE of THF (9.40 ± 0.02 eV) is an upper limit for the RE of [NH_3, H_2O]$^{\bullet+}$. From these two limits, the RE of [NH_3, H_2O]$^{\bullet+}$ is measured for the first time by these bracketing experiments at −9.38 ± 0.04 eV.

Finally, it is of interest to compare this experimental RE value, considered as the opposite of the adiabatic IE of the neutral solvated dimer to the IE value of NH_3, which is 10.07 eV.[34] Solvation by a water molecule reduces the ionization energy by 0.69 eV. This can be related to the neutral and ionized ammonia solvation energies: according to Scheme 1, $\Delta H_{solv}(NH_3^{\bullet+}) - \Delta H_{solv}(NH_3) = -15.9$ kcal mol^{-1}. This value is a measurement of the improved stabilization of a charged species by water as compared to the neutral species. Unfortunately, at least one experimental value would be necessary to relate the result of this measurement to the heat of formation of $NH_3 + H_2O$ or to that of $NH_3^{\bullet+} + H_2O$, but we are not aware of any experimental measurement of the solvation energies of ammonia.

Proton Transfer Reactions. As the charge transfer pathway has been probed by neutrals of varying IE, the proton transfer reactions have been probed by a set of bases of different proton affinities. An initial examination of the data presented in Table 3, using the tabulated PA values[35] showed a discrepancy: proton transfer was not observed for the reaction with 4-fluoroacetophenone (PA 205.2 kcal mol^{-1}), whereas it was observed with 1,2-dimethoxyethane (PA 205.1 kcal mol^{-1}) and *N*-methylformamide (PA 203.2 kcal mol^{-1}), which present a lower proton affinity. This led us to question the published PA values for two of these species (*N*-methylformamide and 4-fluoro-

TABLE 4: ab Initio Calculation Energies for the Different Charge Transfer and Proton Transfer Reactant and Product Species, Computed Both on MP2/6-31G and B3LYP/6-31G** Optimized Structures**

	MP2/6-31G** geometry							B3LYP/6-31G** geometry	
	G3(MP2)				CCSD(T)/aug-cc-pVTZ			CCSD(T)/aug-cc-pVTZ	
species	E (Hartrees)	ΔE_{0K} (eV)[a]	ΔH_{298K} (kcal mol^{-1})[b]	ΔG_{298K} (kcal mol^{-1})[b]	E (Hartrees)	ΔE_{0K} (eV)[a]	ΔH_{298K} (kcal mol^{-1})[b]	E (Hartrees)	ΔE_{0K} (eV)[a]
$[NH_3, H_2O]^{\bullet+}$	−132.458761	0.00	0.0	0.0	−132.488224	0.00	0.0	−132.487461	0.00
$[NH_3, H_2O]$ (vertical)[c]	−132.765880	−8.36			−132.802406	−8.55		−132.795424	−8.36
$[NH_3, H_2O]$	−132.802098	−9.34			−132.833350	−9.39		−132.833300	−9.41
$[NH_3, H_2O]^{\bullet+}$ (vertical)[d]	−132.383401	2.05			−132.412431	2.06		−132.413087	2.02
$NH_3 + H_2O$	−132.791953	−9.07			−132.822861	−9.11		−132.822825	−9.13
$[NH_2^{\bullet}, H_2O] + H^+$	−132.116948		205.3	196.7	−132.146688		205.3	−132.146450	
$[NH_3, OH^{\bullet}] + H^+$	−132.108485		214.4	207.8	−132.138691		213.9	−132.138608	
$NH_2^{\bullet} + H_2O + H^+$	−132.112686		208.8	194.8	−132.142156		208.8	−132.142084	
$OH^{\bullet} + NH_3 + H^+$	−132.096594		220.1	206.4	−132.126123		220.1	−132.126078	
$NH_3^{\bullet+} + H_2O$	−132.421777	1.01	22.3	15.1	−132.449979	1.04	23.1	−132.449905	

[a] Relative to $[NH_3, H_2O]^{\bullet+}$, these values correspond to the recombination energy for relevant transitions. [b] Relative to $[NH_3, H_2O]^{\bullet+}$, these values are directly related to the proton affinity and gas-phase basicity scales. [c] Neutral energy computed on the optimized $[NH_3, H_2O]^{\bullet+}$ geometries. [d] Ionized energy computed on the optimized neutral $[NH_3, H_2O]$ geometries.

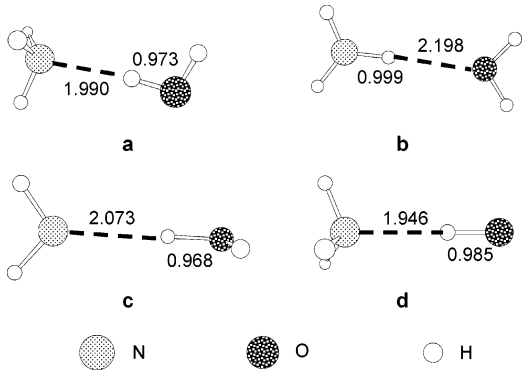

Figure 3. Ab initio molecular-orbital optimized structures (at the MP2/6-31G** level of the theory) of the dimers. a, $[NH_3, H_2O]$; b, $[NH_3, H_2O]^{\bullet+}$; c, $[NH_2^{\bullet}, H_2O]$; d, $[NH_3, OH^{\bullet}]$. (Distances in angstroms.)

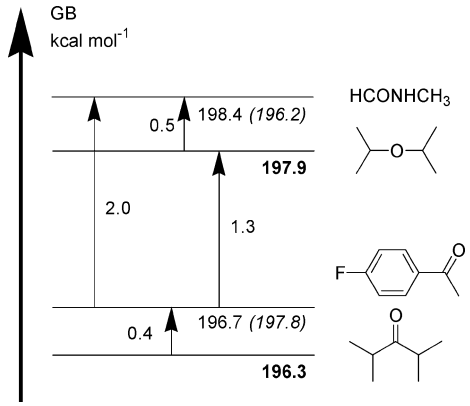

Figure 4. Experimental relative gas-phase basicities between *N*-methylformamide, diisopropyl ether, diisopropyl ketone, and 4-fluoroacetophenone. Arrows indicate relative GB as measured by the equilibrium method. The GB of the reference bases are in bold font; the reevaluated GB is followed by the previous value in italics. (Error margin is ±0.2 kcal mol^{-1}.)

acetophenone). The gas-phase basicities (GB) of *N*-methylformamide and 4-fluoroacetophenone relative to two reference bases, diisopropyl ether (GB 197.9 kcal mol^{-1}) and diisopropyl ketone (GB 196.3 kcal mol^{-1}) were therefore measured in the FT-ICR instrument by the standard equilibrium method.[48] The measurements yielded the consistent relative gas-phase basicity ladder presented in Figure 4, which shows that, contrary to the tabulated values, *N*-methylformamide is more basic than 4-fluoroacetophenone. As a consequence, the gas-phase basicities and proton affinities are revised for *N*-methylformamide (GB 198.4 kcal mol^{-1}, PA 205.9 kcal mol^{-1}) and for 4-fluoroacetophenone (GB 196.7 kcal mol^{-1}, PA 203.8 kcal mol^{-1}).

These revised proton affinity values give a consistent result for the proton transfer pathway: the threshold for the proton transfer channel occurs for bases with a PA between 203.8 and 205.1 kcal mol^{-1}. As for the charge transfer pathway, the first problem is to determine the neutral reaction products, as four reaction products could be formed: $[NH_2^{\bullet}, H_2O]$, $[NH_3, OH^{\bullet}]$, $NH_2^{\bullet} + H_2O$, or $NH_3 + OH^{\bullet}$. The examination of the bond dissociation energies (BDEs)[49] for the loss of $H^{\bullet}$ for NH_3 (BDE = 108.7 kcal mol^{-1}) and for H_2O (BDE = 119.3 kcal mol^{-1}) clearly indicate that, for the nonsolvated neutrals, the thermodynamically most favorable pathway is the formation of $NH_2^{\bullet} + H_2O$. The authors are not aware of any data on the solvation energy of the $NH_2^{\bullet}$ radical by water or of the $OH^{\bullet}$ radical by ammonia. Nevertheless, the formation of a hydrogen bond between two neutral species is usually in the range of 2−5 kcal mol^{-1}, which is much less than the difference between the formation of $NH_2^{\bullet}$ and $OH^{\bullet}$. It is therefore likely that either $[NH_2^{\bullet}, H_2O]$ or $NH_2^{\bullet} + H_2O$ is formed by the proton transfer reaction.

The observation of a pathway which proceeds through a loss of $NH_2^{\bullet}$ for neutrals for which the PA is slightly lower than the proton transfer threshold (e.g., methyl propanoate, methyl butanoate, diethyl ether) also supports this result: $NH_2^{\bullet}$ is probably formed in an intermediate complex which possess enough energy to undergo the proton transfer reaction from $NH_3^{\bullet+}$ to the neutral base, but not enough energy to completely dissociate. It is not possible to conclude whether this threshold corresponds to the formation of the $[NH_2^{\bullet}, H_2O]$ solvated radical or to the complete dissociation to $NH_2^{\bullet} + H_2O$. The calculation results (Table 4) shed some light on this point: according to these, if the reaction led to full dissociation, the reaction should not occur with bases of PA lower than 208.8 kcal mol^{-1}. Because proton transfer is observed for *N*-methylformamide and 1,2-dimethoxyethane, it seems possible that the proton transfer ends up with the formation of a water-solvated $NH_2^{\bullet}$ radical. As for the formation of the water−ammonia dimer, in the thermal conditions of the experiment, it is likely that the dimer will eventually dissociate in a longer time frame. Therefore, the observed threshold is probably a measurement of the proton affinity of the $[NH_2^{\bullet}, H_2O]$ dimer, evaluated at 204.4 ± 0.9 kcal mol^{-1}. This result is also in good agreement with the theoretical PA of 205.3 kcal mol^{-1}.

SCHEME 2

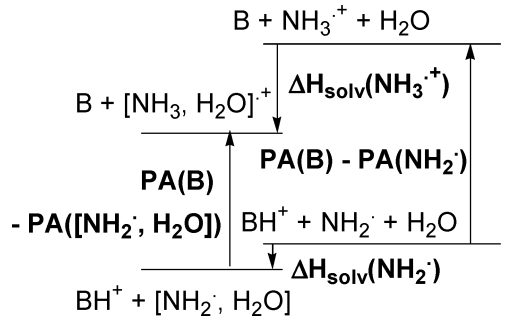

Solvation of the $NH_2^\bullet$ radical by water leads to a 19.6 kcal mol^{-1} increase in proton affinity, from 184.8 to 204.4 kcal mol^{-1}, which can be interpreted in terms of differences in solvation energies (Scheme 2). If one now considers that in the case of the charge transfer the ionization energy was decreased by only 15.9 kcal mol^{-1}, it is obvious that these two measurements do not measure only the ionized ammonia solvation energy. The proton transfer measurement indicates that the ionized ammonia solvation energy is at least 19.6 kcal mol^{-1}; therefore, these two experimental results demonstrate that, in the case of the charge transfer, some energy is gained by the elimination of a bound [NH_3, H_2O] neutral dimer.

Under the hypothesis that a neutral radical dimer is formed, this 19.6 kcal mol^{-1} difference in energy represents the difference between radical and protonated solvation energies (Scheme 2): $\Delta H_{solv}(NH_3^{\bullet+}) - \Delta H_{solv}(NH_2^\bullet) = -19.6$ kcal mol^{-1}; as for the charge transfer measurement, it does not lead to a measurement of the solvation energy of ionized ammonia. The comparison between the value obtained for charge transfer and that for proton transfer makes it obvious that the stabilization of $NH_2^\bullet$ by water is about 3 kcal mol^{-1} less than that of NH_3. This is to be expected, because $NH_2^\bullet$ is an electron-deficient species less prone to be an electron donor in a hydrogen bond than NH_3.

Competition between Charge/Proton Transfer and Other Reaction Pathways. The examination of Tables 1 and 2 shows that for most neutrals other reactions compete with the charge transfer reaction. One can observe an evolution as the IE increases and the branching ratio for the charge transfer pathway decreases: this indicates that the charge transfer pathway becomes less exothermic and therefore less competitive against other pathways. No general trend can be derived, because most neutrals in the IE range under consideration differ widely in their chemical properties. This trend is even more pronounced for the proton transfer reaction: for bases with strong PAs, the only reaction observed is the proton transfer, whereas for bases with a low PA, $H^\bullet$ abstraction is the major channel.

The decrease of the ionization energy for the dimer has consequences for the reactivity: for instance, it was observed[26] that the charge transfer pathway, which is the only reaction product for the reaction of $NH_3^{\bullet+}$ with butanal (IE 9.82 eV[34]), does not occur at all for the [NH_3, H_2O]$^{\bullet+}$ dimer. It is replaced by $H^\bullet$ transfer and a solvated McLafferty-type fragmentation (FR). Solvation therefore modulates the reactivity of the ionized ammonia by opening new reaction channels.

Conclusion

In the present work, two aspects of the reactivity of the [NH_3, H_2O]$^{\bullet+}$ radical cation have been studied: the charge transfer and proton transfer pathways. For both channels, there appears to be a threshold dependence on the ionization energy and proton affinity of the neutral reagents. Under some assumptions about the structure of the neutral reaction products, the thermochemical properties of [NH_3, H_2O]$^{\bullet+}$ can be determined from these measurements. The charge transfer threshold is directly related to the recombination energy of the [NH_3, H_2O]$^{\bullet+}$ dimer, which is, therefore, evaluated at -9.38 ± 0.04 eV. The observed decrease of the ionization energy of ammonia in the solvated dimer (-0.69 eV, -15.9 kcal mol^{-1}) is a measurement of the difference in solvation energies between the neutral and the ionized ammonia−water complexes. These results are supported by ab initio molecular-orbital calculations, which yield close results for these two values. The thermochemical value actually measured by the proton transfer threshold is less obvious. Correspondence between the experimental and calculated results indicate that the threshold could be relative to the formation of the [$NH_2^\bullet$, H_2O] solvated radical. As in the case of charge transfer, the observed increase in the proton affinity ($+19.6$ kcal mol^{-1}) is a measurement of the difference in solvation energies between ionized ammonia and the $NH_2^\bullet$ radical. A combination of these results show that the ionized ammonia solvation energy is at least 19.6 kcal mol^{-1} and that the difference between the solvation energies of $NH_2^\bullet$ and NH_3 is about 3 kcal mol^{-1}. The G3(MP2) calculations lead to values close to these results: $\Delta H_{solv}(NH_3^{\bullet+}) = -22.3$ kcal mol^{-1}, $\Delta H_{solv}(NH_3) = -6.2$ kcal mol^{-1}, $\Delta H_{solv}(NH_2^\bullet) = -3.5$ kcal mol^{-1}. But the measurement of one of these values would be needed to determine absolute solvation energies for all of these species.

It is of interest to compare these experimental values to those obtained[14] for the ionized water dimer radical cation $(H_2O)_2^{\bullet+}$. In this case, the most stable structure is the dissymmetric [H_3O^+, $OH^\bullet$], but it lies close in energy to the symmetric $3e^-/2c$ dimer structure. The measurement of the recombination energy of the ionized water dimer (10.81 eV) and an estimate of the proton transfer threshold (187.4 kcal mol^{-1}) both indicate that the interaction energy in the water dimer is on the order of 41−46 kcal mol^{-1}. This is about twice the strength of the interaction observed for the [NH_3, H_2O]$^{\bullet+}$ dimer. This difference can be compared to the empirical relationship established by McMahon for the interaction between proton-bound dimers bound by oxygen atoms[50] ($\Delta H_{PBD} = -125 + {}^1/_2|AP_1 - AP_2|$kJ mol^{-1}): the system is better stabilized when the affinity for the proton is comparable for both moieties of the dimer. A similar trend could exist for radical cation dimers: when both moieties are close in ionization energies, the charge is shared evenly between both. In a system with differing ionization energies for both constituents of the ionized dimer, the charge is more strongly localized on the molecule with the lowest IE. This leads to a lower stabilization energy for the system.

Finally, one should point out that this study has only drawn a partial picture of the complex reactivity of the ionized ammonia dimer: from the experimental results, it is obvious that charge and proton transfer channels are only a part of the various competing channels. Some of the other channels present a common initial development, which halts before complete dissociation is reached because of a lack of sufficient internal energy. This is, for instance, the case of the $NH_2^\bullet$ loss pathway, which is clearly related to neutrals possessing a PA slightly below the threshold for proton transfer. Nevertheless, other reaction products, such as the fragmentation of linear or cyclic ethers, cannot be rationalized so easily. Further work will focus on these unusual reaction pathways.

Acknowledgment. The authors would like to thank H. E. Audier and P. Mourgues for helpful discussions in the preparation of this manuscript. They also thank the CNRS for financial support of this work.

References and Notes

(1) van der Rest, G.; Mourgues, P.; Nedev, H.; Audier, H. E. *J. Am. Chem. Soc.* **2002**, *124*, 5561.
(2) Engdahl, A.; Nelander, B. *J. Chem. Phys.* **1989**, *91*, 6604.
(3) Yeo, G. A.; Ford, T. A. *Spectrochim. Acta, Part A* **1991**, *47*, 485.
(4) Fraser, G. T.; Suenram, R. D. *J. Chem. Phys.* **1992**, *96*, 7287.
(5) Stockman, P. A.; Bumgarner, R. E.; Suzuki, S.; Blake, G. A. *J. Chem. Phys.* **1992**, *96*, 2496.
(6) Herbine, P.; Dyke, T. R. *J. Chem. Phys.* **1985**, *83*, 3768.
(7) Sadlej, J.; Moszynski, R.; Dobrowolski, J. C.; Mazurek, A. P. *J. Phys. Chem. A* **1999**, *103*, 8528.
(8) Rzepkowska, J.; Uras, N.; Sadlej, J.; Buch, V. *J. Phys. Chem. A* **2002**, *106*, 1790.
(9) Sodupe, M.; Oliva, A.; Bertran, J. *J. Am. Chem. Soc.* **1994**, *116*, 8249.
(10) Tachibana, A.; Kawauchi, S.; Nakamura, K.; Inaba, H. *Int. J. Quantum Chem.* **1996**, *57*, 673.
(11) Ng, C. Y.; Trevor, D. J.; Tiedemann, P. W.; Ceyer, S. T.; Kronebusch, P. L.; Mahan, B. H.; Lee, Y. T. *J. Chem. Phys.* **1977**, *67*, 4235.
(12) Norwood, K.; Ali, A.; Ng, C. Y. *J. Chem. Phys.* **1991**, *95*, 8029.
(13) Giles, K.; Adams, N. G.; Smith, D. *J. Phys. B* **1989**, *22*, 883.
(14) de Visser, S. P.; de Koning, L. J.; Nibbering, N. M. M. *J. Phys. Chem.* **1995**, *99*, 15444.
(15) van der Rest, G.; Chamot-Rooke, J.; Mourgues, P.; McMahon, T. B.; Audier, H. E. *J. Am. Soc. Mass Spectrom.* **2001**, *12*, 938.
(16) Gauld, J. W.; Radom, L. *J. Am. Chem. Soc.* **1997**, *119*, 9831.
(17) Audier, H. E.; Mourgues, P.; van der Rest, G.; Chamot-Rooke, J.; Nedev, H. Catalyzed Isomerizations of Ions in the Gas Phase. In *Advances in Mass Spectrometry*; Gelpi, E., Ed.; Wiley: Chichester, 2001; Vol. 15, pp 101.
(18) Trikoupis, M. A.; Burgers, P. C.; Ruttink, P. J. A.; Terlouw, J. K. *Int. J. Mass Spectrom.* **2002**, *217*, 97.
(19) van der Rest, G.; Mourgues, P.; Audier, H. E. *Int. J. Mass Spectrom.* **2004**, *231*, 83.
(20) Wong, C. Y.; Ruttink, R. J. A.; Burgers, P. C.; Terlouw, J. K. *Chem. Phys. Lett.* **2004**, *390*, 176.
(21) Audier, H. E.; Leblanc, D.; Mourgues, P.; McMahon, T. B.; Hammerum, S. *J. Chem. Soc., Chem. Commun.* **1994**, 2329.
(22) Cao, J.; Tu, Y.-P.; Sun, W.; Holmes, J. L. *Int. J. Mass Spectrom.* **2003**, *222*, 41.
(23) van der Rest, G.; Nedev, H.; Chamot-Rooke, J.; Mourgues, P.; McMahon, T. B.; Audier, H. E. *Int. J. Mass Spectrom.* **2000**, *202*, 161.
(24) Trikoupis, M. A.; Burgers, P. C.; Ruttink, P. J. A.; Terlouw, J. K. *Int. J. Mass Spectrom.* **2001**, *210/211*, 489.
(25) Troude, V.; van der Rest, G.; Mourgues, P.; Audier, H. E. *J. Am. Chem. Soc.* **1997**, *119*, 9287.
(26) van der Rest, G.; Jensen, L. B.; Abdel Azeim, S.; Mourgues, P.; Audier, H. E. *J. Am. Soc. Mass Spectrom.* **2004**, *15*, 966.
(27) Allemann, M.; Kellerhals, H.; Wanczek, K. P. *Int. J. Mass Spectrom. Ion Phys.* **1983**, *46*, 139.
(28) Kofel, P.; Allemann, M.; Kellerhals, H.; Wanczek, K. P. *Int. J. Mass Spectrom. Ion Processes* **1985**, *65*, 97.
(29) Caravatti, P.; Allemann, M. *Org. Mass Spectrom.* **1991**, *26*, 514.
(30) Flammang, R.; Nguyen, M. T.; Bouchoux, G.; Gerbaux, P. *Int. J. Mass Spectrom.* **2000**, *202*, A8.
(31) Bartmess, J. E.; Georgiadis, R. M. *Vacuum* **1983**, *33*, 149.
(32) Miller, K. J.; Sacvhik, J. A. *J. Am. Chem. Soc.* **1979**, *101*, 7206.
(33) Su, T.; Chesnavich, W. J. *J. Chem. Phys.* **1982**, *76*, 5183.
(34) Lias, S. G. Evaluated ionization energies. In *NIST Chemistry Webbook, NIST Standard Reference Database Number 69*; Lindstrom, P. J., Mallard, W., Eds.; National Institute of Standards and Technology: Gaithersburg, MD, 20899; 2003 (http://webbook.nist.gov).
(35) Hunter, E. P.; Lias, S. G. Proton affinity evaluation. In *NIST Chemistry Webbook, NIST Standard Reference Database Number 69*; Lindstrom, P. J., Mallard, W., Eds.; National Institute of Standards and Technology: Gaithersburg, MD, 20899; 2003 (http://webbook.nist.gov).
(36) Frisch, M. J.; Trucks, G. W.; Schlegel, H. B.; Scuseria, G. E.; Robb, M. A.; Cheeseman, J. R.; Zakrzewski, V. G.; Montgomery, J. A., Jr.; Stratmann, R. E.; Burant, J. C.; Dapprich, S.; Millam, J. M.; Daniels, A. D.; Kudin, K. N.; Strain, M. C.; Farkas, O.; Tomasi, J.; Barone, V.; Cossi, M.; Cammi, R.; Mennucci, B.; Pomelli, C.; Adamo, C.; Clifford, S.; Ochterski, J.; Petersson, G. A.; Ayala, P. Y.; Cui, Q.; Morokuma, K.; Malick, D. K.; Rabuck, A. D.; Raghavachari, K.; Foresman, J. B.; Cioslowski, J.; Ortiz, J. V.; Stefanov, B. B.; Liu, G.; Liashenko, A.; Piskorz, P.; Komaromi, I.; Gomperts, R.; Martin, R. L.; Fox, D. J.; Keith, T.; Al-Laham, M. A.; Peng, C. Y.; Nanayakkara, A.; Gonzalez, C.; Challacombe, M.; Gill, P. M. W.; Johnson, B. G.; Chen, W.; Wong, M. W.; Andres, J. L.; Head-Gordon, M.; Replogle, E. S.; Pople, J. A. *Gaussian 98*; Gaussian, Inc.: Pittsburgh, PA, 1998.
(37) Curtiss, L. A.; Redfern, P. C.; Raghavachari, K.; Rassolov, V.; Pople, J. A. *J. Chem. Phys.* **1999**, *110*, 4703.
(38) Brutschy, B.; Eggert, J.; Janes, C.; Baumgärtel, H. *J. Phys. Chem.* **1991**, *95*, 5041.
(39) Grover, J. R.; Cheng, B.-M.; Herron, W. J.; Coolbauch, M. T.; Peifer, W. R.; Garvey, J. F. *J. Phys. Chem.* **1994**, *98*, 7479.
(40) Dedonder-Lardeux, C.; Jouvet, C.; Martrenchard-Barra, S.; Solgadi, D.; Dimicoli, I. *Chem. Phys. Lett.* **1997**, *264*, 595.
(41) Thölmann, D.; Grützmacher, H. F. *Chem. Phys. Lett.* **1989**, *163*, 225.
(42) Thölmann, D.; Grützmacher, H. F. *J. Am. Chem. Soc.* **1991**, *113*, 3281.
(43) Lias, S. G.; Ausloos, P. J. *J. Am. Chem. Soc.* **1978**, *100*, 6027.
(44) Hunter, E. P. L.; Lias, S. G. *J. Phys. Chem. Ref. Data* **1998**, *27*, 413.
(45) Lias, S. G.; Ausloos, P. J.; Horvath, Z. *Int. J. Chem. Kinet.* **1976**, *8*, 725.
(46) Sieck, L. W.; Ausloos, P. J. *J. Chem. Phys.* **1990**, *93*, 8374.
(47) Bouchoux, G.; Leblanc, D.; Sablier, M. *Int. J. Mass Spectrom.* **2001**, *210*, 189.
(48) McMahon, T. B. *Int. J. Mass Spectrom.* **2000**, *200*, 187.
(49) Afeefy, H. Y.; Liebman, J. F.; Stein, S. E. Neutral Thermochemical Data. In *NIST Chemistry Webbook, NIST Standard Reference Database Number 69*; Lindstrom, P. J., Mallard, W., Eds.; National Institute of Standards and Technology: Gaithersburg, MD, 20899; 2003 (http://webbook.nist.gov).
(50) Larson, J. W.; McMahon, T. B. *J. Am. Chem. Soc.* **1982**, *104*, 6255.